VOL. 11, NO. 22, NOVEMBER 2016 ISSN 1819-6608
ARPN Journal of Engineering and Applied Sciences

www.arpnjournals.com

INVESTIGATIONS INTO THE EFFECTS OF MAXIMUM DEFLEXTION IN LOW STIFFNESS RESILIENT SHAFT OF SEMI ACTIVE STEERING SYSTEMS

Roslina Ab. Rashid, Joga D. Setiawan, Mui'nuddin Maharun and Masri B. Baharom
Department of Mechanical Engineering, Bandar Seri Iskandar Perak, Malaysia
E-Mail: joga.setiawan@petronas.com.my

ABSTRACT

The objective of this research was to examine the effects of low-stiffness-resilient-shaft (LSRS) maximum deflection angle on the response of a vehicle equipped with Semi Active Steering System (SAS) during the failure of Steer-by-wire (SBW). Modelling of LSRS stiffness that considers deflection angle was proposed and incorporated to the 3-DOF bicycle model of the vehicle dynamic. Simulations were performed on MATLAB/SIMULINK for several vehicle longitudinal speeds and the LSRS maximum deflection angles by applying a standard step steer input. Simulation results showed that vehicle responses were considered safe from roll over problem during the specified cornering maneuver since the lateral acceleration and yaw velocity values of the SAS system were always lower than the ones of the conventional systems. The turning radius was found to increase as the maximum deflection angle increased. However, the turning radius became constant after a certain maximum deflection angle was used. The maximum deflection angle of LSRS to be as low as possible, between 10º to 30º was suggested for keeping a consistent vehicle's drivability.

Keywords: steer-by-wire, simulation, safety, stability, drivability, automotive.

INTRODUCTION

Steering system is another contributing factor that plays a role to the enhancement of passenger safety as well as vehicle stability. Steering system is the key interface between driver and the vehicle. Therefore, the reliable steering system is required during normal driving condition or negotiating the corner as well as avoiding the occurrence of accident.

Steer-by-wire (SBW) one of the latest creation in vehicle industry with a lots of benefits such as the weight of the vehicle are reduced and less injury during the front-end collision [1]. SBW system operates by replacing the rigid steering shaft with electronic controllers. However, system that fully relies on electronics circuit has critical challenge to maintain its functionality during the unexpected condition [2]. The main concern is to ensure the safety of the driver and passengers in the event of steering failure.

However, there are limited safety backup for SBW during the failure. Some other researcher proposed using a clutch, and servo motor as a backup [2, 3]. Concern to this problem, Semi-active-steering (SAS) system was introduced as a replacement to the SBW system during SBW system failure. SAS operates similarly as SBW with providing all the benefits together with backup system by replacing the clutch system with low-stiffness-resilient-shaft (LSRS) as a backup in the event of SBW failure. LSRS as shown in Figure-1 is attached permanently between the steering wheel and the pinion gear. It will operate as a conventional steering system in the event of SBW system failure. Several previous studies proved that LSRS is safe to be driven in the event of SBW failure [4, 5].

This paper examines the effect of maximum deflection of the LSRS to the response of the vehicle during a standard cornering maneuver in which a constant steering angle of 90º is maintained. This study which has never been available in the literature, is important for ensuring the stability and handling performance of vehicle during the design stage of LSRS. The vehicle dynamic response to the applied steering angle input is analysed by utilizing the three degree-of-freedom (3-DOF) bicycle model as shown in Figure-2. The stiffness of LSRSS is modelled to be constant when the deflection is less than about 80 % of the maximum deflection. The stiffness parameter is modelled to follow a tangent hyperbolic function tin which its value increases continuously fast after this point. Simulations were performed to provide the vehicle position on a plane, lateral velocity, longitudinal velocity, lateral acceleration, and yaw velocity. The turning radius of the vehicle during this maneuver is estimated at various initial longitudinal speeds v_x and maximum deflection of LSRS Δ_o.

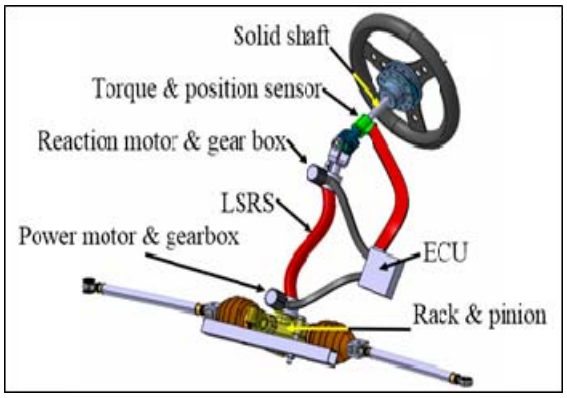

Figure-1. Semi active steering system (SAS) including SBW and LSRS.

MATHEMATICAL MODEL

The non-linear 3-DOF model used for analysis is based on diagram in Figure-2 which is from reference [7]. The nomenclature used in defining the major variables and geometric parameters of the model is given at the end of report. The dynamics of lateral and longitudinal vehicle motion when a vehicle is running with zero acceleration F_x are described allowing the longitudinal velocity v_x to vary due to the non-zero values of lateral velocity v_y and yaw velocity r.

$$\dot{v}_x = \frac{F_x}{m} + r v_y \quad (1)$$

$$\dot{v}_y = \frac{1}{mv_x}(-aC_{cf} + bC_{cr})r - \frac{1}{mv_x}(C_{cf} + C_{cr})v_y + \frac{1}{m}C_{cf}\delta_F - r v_x \quad (2)$$

$$\dot{r} = \frac{1}{I_{zz}v_x}(-a^2C_{cf} - b^2C_{cr})r - \frac{1}{I_{zz}v_x}(aC_{cf} - bC_{cr})v_y + \frac{1}{I_{zz}}aC_{cf}\delta_F \quad (3)$$

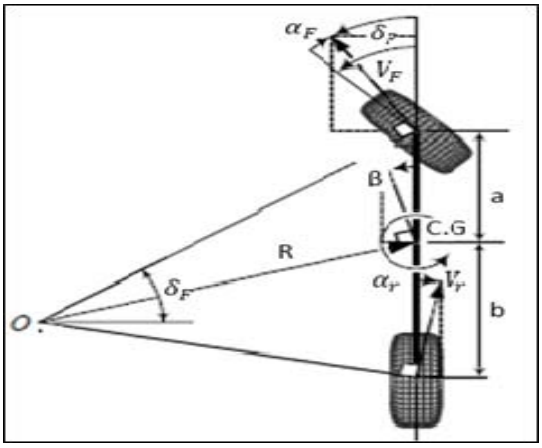

Figure-2. 3DOF bicycle model [7].

After finding the translational and rotational velocities of the vehicle v_x, v_y, and r, the path of motion for the vehicle is determined by integration as follows.

$$\psi = \psi_0 + \int r\,dt \quad (4)$$

$$x = \int (v_x \cos\psi - v_y \sin\psi)\,dt \quad (5)$$

$$y = \int (v_x \cos\psi + v_y \sin\psi)\,dt \quad (6)$$

The SAS system model during failure of SBW, adopted from Baharom et. al [6] is shown in Figure-3 with the detailed of its free body diagram. The relationship between the steering wheel angle δ_{sw} as the input and the average front wheel angle δ_F as the output can be derived.

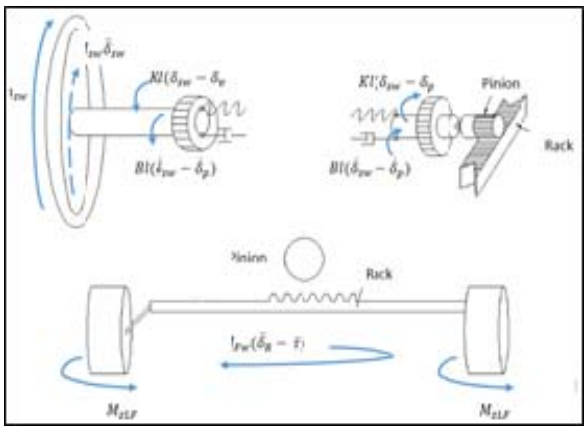

Figure-3. Free-body diagram of SAS during system failure.

$$\delta_g = G\delta_F \quad (7)$$

$$I_{FW}(\ddot{\delta}_F + \ddot{t}) = G\left(\left(\ddot{\delta}_{SW} - \ddot{\delta}_g\right) + K_l\left(\delta_{SW} - \delta_g\right)\right) - B_{FW}\dot{\delta}_F - \tau_f - M_{sf} \quad (8)$$

where

$$\tau_f = F_{cf}\,sgn(\dot{\delta}_F) \quad (9)$$

$$M_{sf} = C_{MaF}\alpha_F = C_{MaF}\left(\delta_F - \beta - \frac{ar}{V_x}\right) \quad (10)$$

After rearranging the equation (8), substituting equation (10) and assuming the friction torque to be negligible, the by steering dynamic equation becomes:

$$G(B_l\dot{\delta}_{SW} + K_l\delta_{SW}) = I_{FW}\ddot{\delta}_F + (B_{FW} + G^2B_l)\dot{\delta}_F + (C_{MaF} + G^2K_l)\delta_F - C_{MaF}\beta - \frac{aC_{MaF}}{v_x}r + I_{FW}\ddot{t} \quad (11)$$

The main feature of this study is the incorporation of non-constant LSRS stiffness K_l formulated in Equation (12). Using minimum stiffness K_{l0} = 5 Nm/rad and the constant value of K = 1000 Nm/rad, the curves of K_l for maximum deflection angle or maximum angle of twist Δ_0 of 10° and 30° are presented in Figure-4. The importance of maximum angle of twist was mentioned reference by Baharom et. al [6], however the effect of this parameter was not included in its modelling and analysis.

$$K_l = K_{l0} + K\left[1 + \tanh(|\Delta| - \Delta_0)\right] \quad (12)$$

Noted that in Equation (12), the value of K_l depends on LSRS deflection angle which is the difference between the steering wheel angle and the pinion rotation angle defined as Δ.

$$\Delta = \delta_{SW} - \delta_F = \delta_{SW} - G\delta_F \quad (13)$$

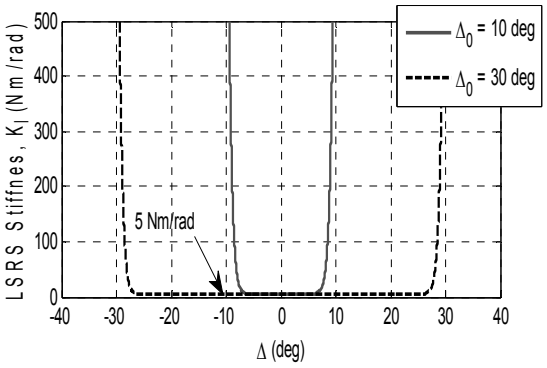

Figure-4. LSRS stiffness model for two different maximum deflection angles Δ_0

SIMULATION RESULTS

Simulations have been set-up on MATLAB/SIMULINK using the Equations (1 to 13) as shown in Figure-5 and the parameters shown in Table-1. Simulations were run for a selected steering wheel input angle referred as 'step steer' [5]. For validation, initial longitudinal velocity V_x of 50 km/h was used to compare between the Yaw Velocities of the new 3-DOF bicycle model to the ones in the previous results in [5]. It can be seen in Figure-6 that the Yaw Velocity of conventional system (rigid shaft) from the previous work [5] is very close to the one using the new model in which both steady state values are about 20 deg/s. For the new model with SAS system, the LSRS maximum deflection angle Δ_0 of 30º was used for sumulation. As shown in Figure-6, labelled as "SAS", the new model results to a higher steady state value (15 deg/s) compared to the previous work result (11 deg/s), labelled as "SAS [5]".

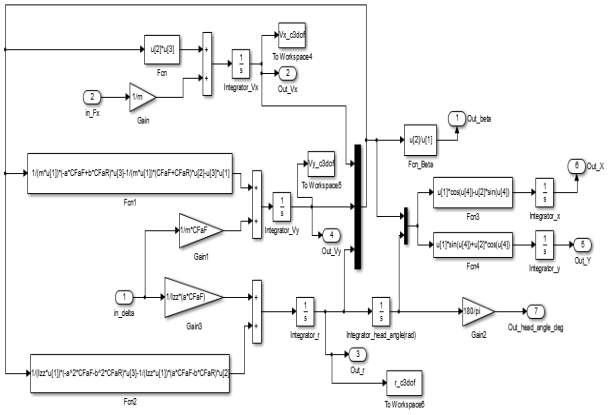

Figure-5. Simulink diagram of 3DOF bicycle model for SAS simulation.

Table-1. Simulation Parameters.

Parameter	Value	Unit
a	1.02	m
b	1.48	m
m	1200	Kg
B_{Fw}	800	N.m.s/rad
$C_{\alpha f}$	40279	N/rad
$C_{\alpha r}$	40279	N/rad
$C_{M\alpha F}$	1177.1	N.m/rad
G	17	-
I_{zz}	1552	kg.m^2
I_{Fw}	2.0	kg.m^2

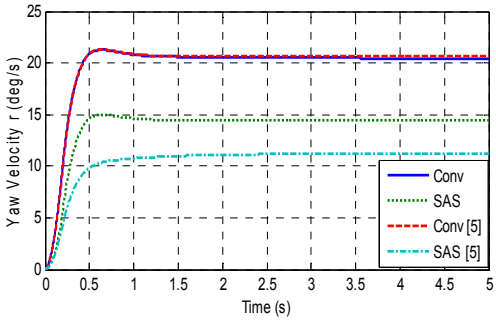

Figure-6. Comparison of Yaw velocities for the new 3-DOF model vs the previous results [5]

Furthermore, simulation was performed using the new model with initial longitudinal velocity V_x of 30 km/h and LSRS maximum deflection Δ_0 of 30º. The results are presented in Figures-7 to 10. In this case simulation of SAS system response during the failure of SBW is compared to the conventional system such as using a rigid shaft.

Figure-7(a) shows the trajectory the steering wheel angle as the input, starting from 0 then suddenly it increases to 90º within 0.2 s and remains at 90º for the rest of simulation that ends at 15 s. It can be seen in Figure-7(b) that the front wheel angle of the SAS system reaches its steady state value of 3.9º while angle of the conventional system reaches the steady state value at around 5.5º. At the same time the longitudinal speed V_x for both SAS and the conventional systems drift slightly from its initial value of 8.33 m/s (30 km/h) as shown in Figure-7(c). The lateral speed V_y of both cases seems to converge to around 0.13 m/s after 15 s as seen in Figure-7(d).

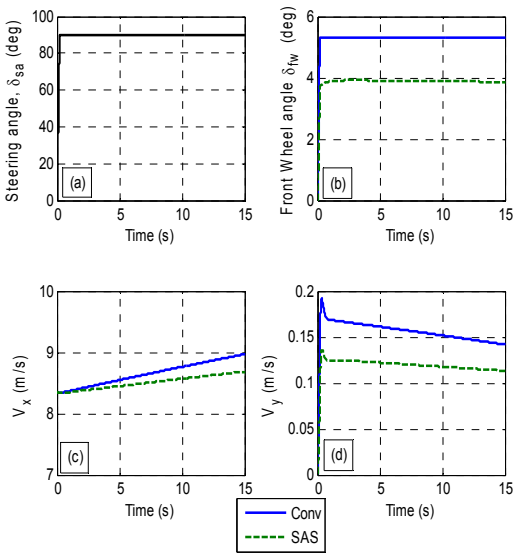

Figure-7. (a) Steering angle, (b) Front wheel angle, (c) Longitudinal speed, and (d) Lateral speed using Δ_0= 30º.

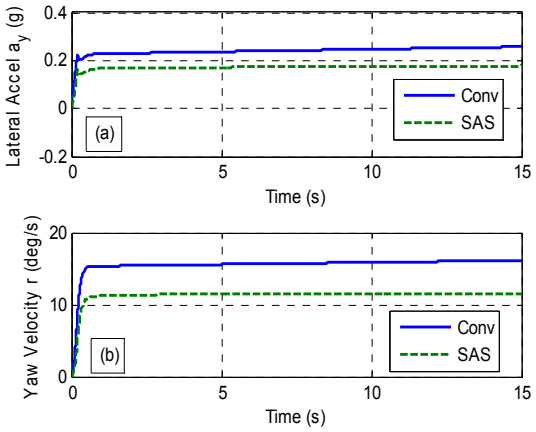

Figure-8. (a) Lateral acceleration, and (b) Yaw velocity using Δ_0= 30º

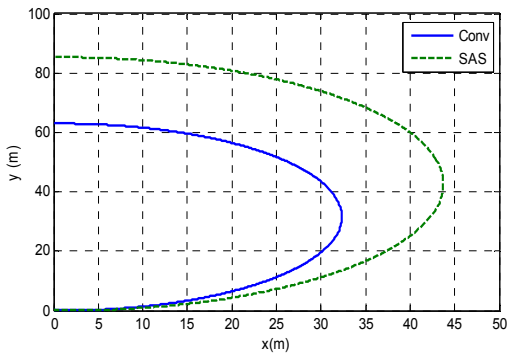

Figure-9. Translational motion using Δ_0= 30º.

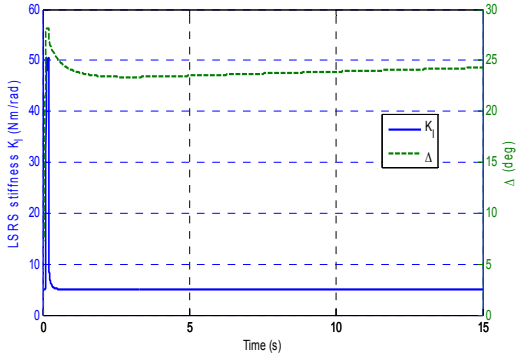

Figure-10. LSRS stiffness and deflection angle using Δ_0= 30º.

The lateral acceleration a_y and yaw velocity r for SAS systems are always lower than the ones of conventional systems as shown in Figure-8. Thus the vehicle response is considered to be safe from a rolling case. However, the translational motion of the vehicle with SAS system results to a cornering maneuver with higher turning radius as shown in Figure-9 in which the turning radius of the SAS system is about 42 m while the one of the conventional system is about 31 m.

During this cornering maneuver, the LSRS deflection angle Δ initially increased to 28º at time of 0.2 s causing the stiffness to increase to around 50 Nm/rad as shown in Figure-10. After 0.2 s, the steering angle and stabilize at 24º and 5 Nm/rad consecutively. Two additional cases for Δ_0 of 10º (small) and 60º (large) were performed to analyse the time trace of the LSRS stiffness with respect to the deflection angle Δ. For the small Δ_0, the LSRS deflection angle Δ initially increased to 8.8º at time of 0.2 s causing the stiffness to increase to around 166 Nm/rad as shown in Figure-11. After 0.2 s, the steering angle and stabilize at 7.5º and 20 Nm/rad. For the large Δ_0, as shown in Figure-12 the LSRS deflection angle Δ initially increased to 50º at 0.2 s while the stiffness stayed at 5 Nm/rad.

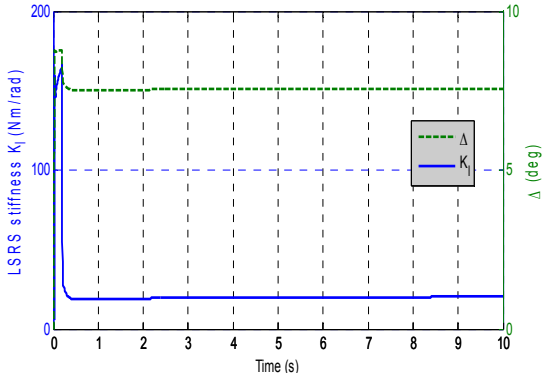

Figure-11. LSRS stiffness and deflection angle using Δ_0 = 10º (considered as 'small').

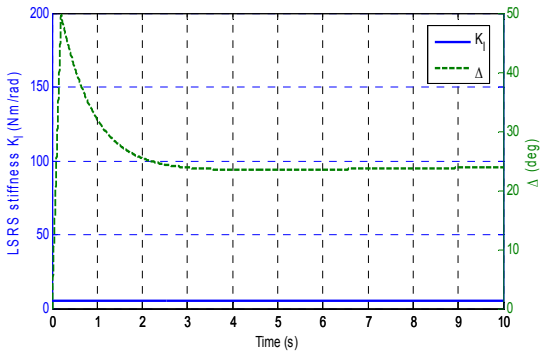

Figure-12. LSRS stiffness and deflection angle using $\Delta_0 = 60^o$ (considered as 'large').

Turning radius of vehicle during this cornering manoeuvre for various initial longitudinal speeds V_x and various LSRS maximum deflection angles Δ_0 are presented in Figure-13. It can be observed that as the turning radius is higher when the LSRS maximum deflection is larger. However, the turning radius will become constant after a certain maximum deflection angle. For example, at longitudinal speed 20 km/h the turning radius becomes constant after the maximum deflection reaches 20º. For smooth transition of driving using SBW to the SAS system it is natural to expect from handling performance view that the increase of turning radius should be as minimum as possible. Thus, the maximum deflection Δ_0 of between 10º to 30º might be optimal.

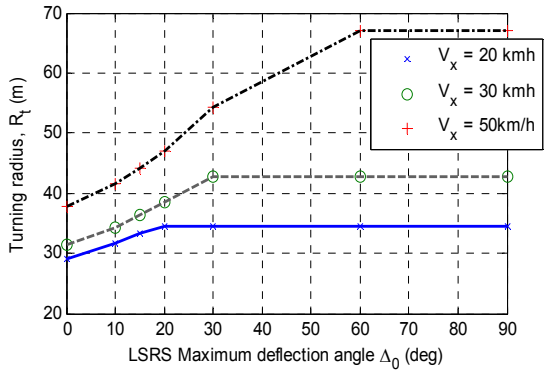

Figure-13. Effect of maximum deflection angle to vehicle's turning radius at various longitudinal speeds

CONCLUSION AND FUTURE WORK

The SAS system with non-constant LSRS stiffness in order to investigate the effect the maximum deflection angle of LSRS has been modelled in conjunction with the 3-DOF bicycle model of vehicle dynamic. Using a standard step steer input, simulations had been performed on MATLAB/SIMULINK for several vehicle longitudinal speeds and the LSRS maximum deflection angles. Simulation results showed that the lateral acceleration and yaw velocity values of the SAS system were always lower than the ones of the conventional system; thus the vehicle is considered safe from roll over problem during the specified cornering maneuver. The turning radius was found to increase as the maximum deflection angle increased. However, the turning radius became constant after a certain maximum deflection angle was used. It is recommended that the maximum deflection angle of LSRS to be as low as possible, between 10º to 30º.

ACKNOWLEDGEMENTS

Authors are thankful to Universiti Teknologi Petronas for providing the resources required for this work.

NOMENCLATURE

a, b	Distant from C.G. to front contact patch, rear contact patch (m)
a_y	Total lateral acceleration (m/s2)
B_l	Steering shaft damping coefficient (Nm.s/rad)
B_{FW}	Front wheel assembly damping coefficient (Nm.s/rad)
$C_{\alpha f}$, $C_{\alpha r}$	Front and rear cornering coefficient (N/rad)
$C_{M\alpha F}$	Self-aligning torque coefficient (N m/rad)
G	steering ratio
I_{FW}	Moment of inertia of front wheel assembly (kgm^2)
I_{zz}	Yaw moment of inertia (m^2)
K_l	Steering shaft torsional stiffness (Nm/rad)
m	Total vehicle mass (kg)
M_{zF}	Self-aligning torque (Nm)
r, ṙ	Yaw velocity (rad/s), yaw acceleration (rad/s2)
V_x	Vehicle longitudinal speed (m/s)
α_F	Front slip angle (rad)
B	Side-slip angle
δ_{SW}	Steering wheel angle (rad)
δ_F	Average front wheel angle (rad)
δ_p	Pinion rotation angle (rad)
τ_f , F_{cf}	Friction torque on steering wheel; friction force (Nm, N)
K_0	LSRS minimum stiffness (Nm/rad)
Δ_0	Maximum LSRS deflection angle (deg)
Δ	LSRS deflection angle (deg)

REFERENCES

[1] T.-J. Park, C.-S. Han, and S.-H. Lee, "Development of the electronic control unit for the rack-actuating steer-by-wire using the hardware-in-the-loop simulation system," Mechatronics, vol. 15, no. 8, pp. 899–918, Oct. 2005.

[2] K. Mogi, T. Sugai, R. Sakurai, And N. Suzuki, "Development of a New Steer-by-wire System," Tech. Rev., no. 79, 2011

[3] R. Hayama, M. Higashi, S. Kawahara, S. Nakano, and H. Kumamoto, "Fault-tolerant automobile steering based on diversity of steer-by-wire, braking and acceleration," Reliab. Eng. Syst. Saf., vol. 95, no. 1, pp. 10–17, Jan. 2010.

[4] K. Hussain, M. B. Baharom, and A. J. Day, "Analysis of the properties of a steering shaft used as a back-up for a steer-by-wire system during system failure," vol. 223, pp. 177–188, 2009.

[5] M. B. Baharom, K. Hussain, and A. J. Day, "Design concepts and analysis of a semi-active steering system for a passenger car.," vol. 223, pp. 283–292, 2009.

[6] Baharom,M.B, Hussain, K., and Day, A.J. "Mathematical modelling of a cornering vehicle fitted with hydraulic-power assisted steering". In proceeding of the FISITA 2006, Japan, 2006, F2006V019.

[7] R.N. Jazar, Vehicle Dynamics: Theory and Application, Springer 2008.

[8] British Standard. Road Vehicles-Lateral Transient Response Test Methods-Open-loop Test Methods. BS ISO 7401:2003.